# Investigation of the Time-Dependent BTI-induced Degradation Distribution for Ring Oscillators in Ultra-Long-Term Stress Conditions

Tomoharu Kishita†, Ryo Kishida††, Kazutoshi Kobayashi†,
† Dept. of Electronics, Kyoto Institute of Technology, Kyoto, Japan
†† Dept. of Electrical and Electronic Engineering, Toyama Prefectural University, Toyama, Japan

***Abstract*— BTI-induced degradation of 65 nm FDSOI ring oscillators (ROs) was measured using a long-term measurement system. Temperature and supply voltage were set to 125°C and a nominal voltage of 1.2 V, respectively. Over a measurement period of 300 days, the average BTI-induced degradation exhibited a power-law behavior. The frequency distributions of 840 ROs transitioned from a Gaussian distribution at the short time to multiple Gaussian distributions at the long time. This shift is attributed to two distinct degradation mechanisms; defects close to the interface and those in proximity to the gate. Although the averaged BTI-induced degradation follows a power-law function. As stress time increased, RTN-induced frequency variations also increased, which makes the frequency distributions wider as stress time.**
***Keywords– BTI, RTN, long-term, ring oscillator, distribution***

## I. Introduction

With the aggressive scaling of semiconductor processes, reliability challenges, particularly aging-related degradations, have become increasingly critical. This is especially true for automotive applications, where the use of highly reliable semiconductors is imperative, making reliability evaluation a mandatory process. Bias Temperature Instability (BTI) is one of the primary reliability concerns.BTI originates from the trapping of charges in defects within the oxide film, which leads to fluctuations in the threshold voltage [1]. In addition, Random Telegraph Noise (RTN) is recognized as one of the contributing causes of BTI [2]. BTI typically occurs in MOSFETs when they are in the ON state. To evaluate aging degradation, accelerated testing is commonly used. These tests involve subjecting devices to elevated voltage and temperature levels to expedite degradation processes. While numerous studies have investigated BTI-induced degradation, most have focused on short-term measurements, typically under 100,000 seconds [3].

For accurate predictions of aging degradation based on short-term results, it is essential to validate whether similar degradation patterns are observed in both short-term accelerated tests and long-term measurements. To achieve this, we developed a long-term measurement system incorporating an FPGA (Field Programmable Gate Array) and an MCU (Microcontroller Unit) to assess the degradation of ring oscillators (ROs). Our previous work [4] presented the results of long-term measurements on 7 nm FinFET ROs, where a decrease in oscillation frequency was observed. However, that study could not provide statistical insights due to the limited number of ROs embedded in the chip.

In this study, we report on the long-term measurement results of 840 ROs fabricated using a 65 nm FDSOI (Fully Depleted Silicon On Insulator) process. These results offer a comprehensive analysis of statistical variations in BTI-induced degradation over an extended period.

## II. Ultra Long-Term Measurement System

The ultra long-term measurement system used in this study, depicted in Figs. 1 and 2, is based on the design presented in [4]. It is consists of an FPGA, an MCU, an external power supply and a constant-temperature oven. To ensure continuous operation even during sudden power outages, the entire system is safeguarded by an uninterruptible power supply (UPS). This configuration enables uninterrupted operation over several months.

While IBM's work [5] pioneered long-term measurements, the system described here provides a stable high-temperature environment and precise temperature control through the use of a constant-temperature oven, ensuring consistent and reliable data collection over extended periods.

## III. Structure of Ring Oscillators

The degradation of ROs fabricated using a 65 nm FDSOI process was evaluated. Each RO consists of 11 stages, as shown in Fig. 3 [6]. Four types of ROs were designed, categorized into two groups: the 2-input NOR RO, affected only by negative BTI (NBTI), and the NAND RO, affected only by positive BTI (PBTI). The reduction type ROs [3] are designed to mitigate the effects of environmental variations by analyzing the difference in results between BTI-RO and BTI-R-RO. When oscillation stops, the NOR or NAND gates are exposed to stress from either NBTI or PBTI, which reduces the oscillation frequency of the corresponding ROs.

The stress voltage depends on the position of the MOSFET in logic gates. If the MOSFET is connected to VDD, the applied voltage stress between the gate and source terminal becomes VDD. Conversely, if the MOSFET is connected to the output primal, the stress voltage becomes $|V_{\mathrm{th}}|$. ROs subjected to higher stress are referred to as BTI-ROs, while those under lower stress are labeled as BTI-R-ROs (where "R" denotes reduction). A total of 840 ROs of all four types, were integrated into a single chip for analysis.

## IV. Measurement Results

The measurement conditions were configured as follows: a nominal operating voltage of 1.2 V for VDD, an ambient temperature of 125°C (the maximum for Grade 1 of the AEC-Q100 standard for automotive semiconductors [7]), an oscillation time of 30 $\mu$s, and a total measurement duration exceeding 300 days. Measurement intervals were progressively increased from 10, 100, 1,000, and 10,000 seconds to a final interval of once every 12 hours (43,200 seconds), as illustrated in Fig. 4.

Fig. 5 presents the degradation rates for the four types of ROs, while Fig. 6 highlights the $V_{\mathrm{th}}$ shifts and their respective fitting results. The NBTI-RO exhibited a degradation rate 1.2 times higher than that of the PBTI-RO, consistent with prior studies of similar structures over short-term measurement periods [3], [8]. Reduction-type ROs showed no degradation for measurement times shorter than 3 $\times 10^6$ seconds, but degradation became apparent beyond this threshold. The difference (denoted as "diff") between BTI-RO and BTI-R-RO degradation effectively mitigated environmental variations.

As shown in Fig. 6, both NBTI and PBTI-induced degradations adhered to power-law functions over the entire measurement period. However, the differences (denoted as "diff") deviated from this trend, saturating after approximately 1 $\times 10^6$ seconds. This indicates that BTI-induced degradation is partially canceled out when differences are considered.

The long-term degradation trend aligns with short-term results, though with a larger time exponent. In this study, the time exponent $n$ for ultra long-term measurements was approximately 1/4, compared to 1/5 for short-term results of the same structure and 1/6 as proposed by other studies on the power-law model [3], [8].

## V. Distribution Changes after Long Period

The minimum, first quartile, median, third quartile, and maximum values of the oscillation frequency of 840 ROs are compared with the mean value. The distributions for measurement times of up to 10,000 seconds and over 16 million

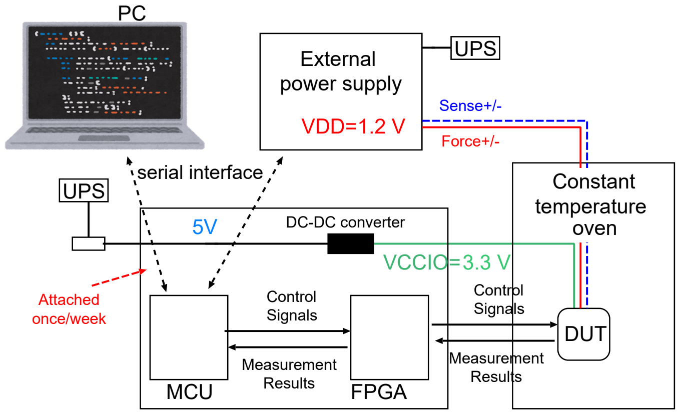


Fig. 1: Long term measurement system [4].

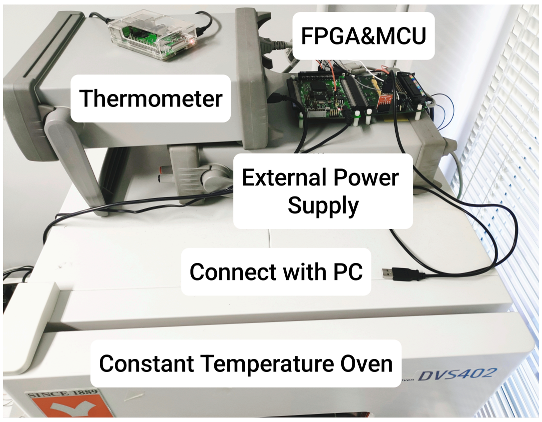


Fig. 2: Photograph of long term measurement system [4].

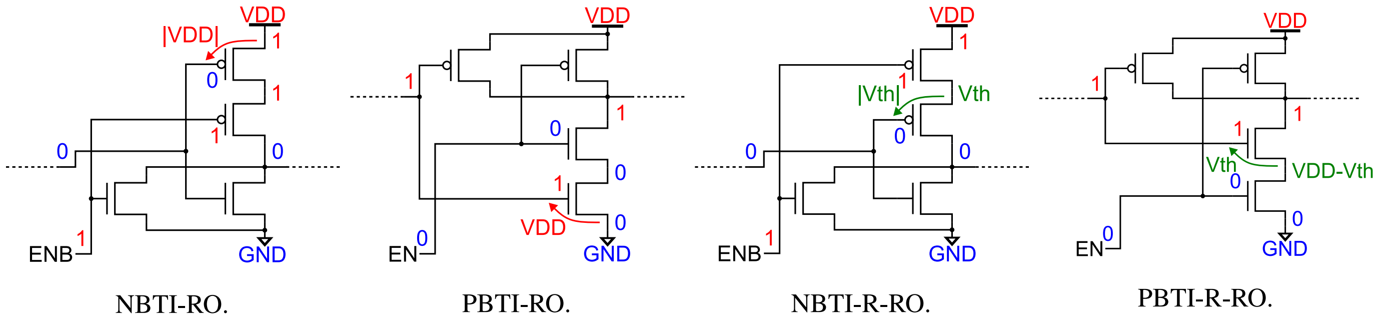


Fig. 3: The schematics of 4 types of ROs [3].

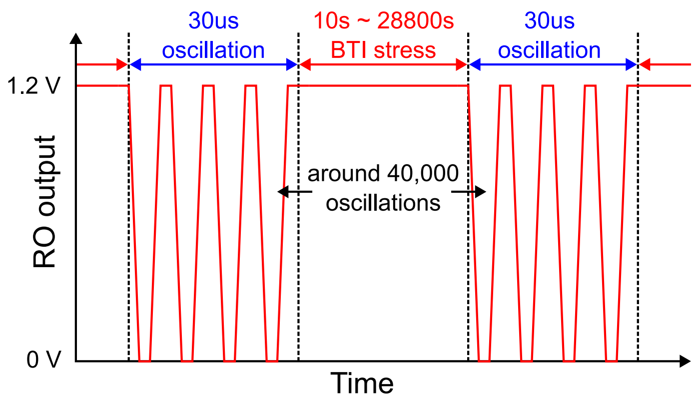


Fig. 4: Measurement method of BTI-induced degradation indicated by RO output

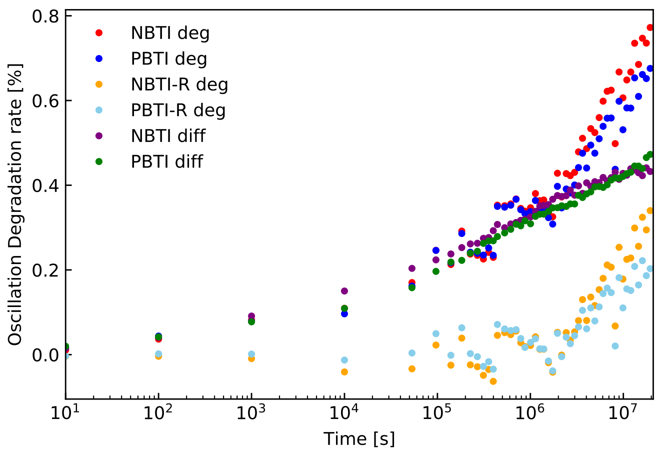


Fig. 5: Degradation rates for all ROs and difference.

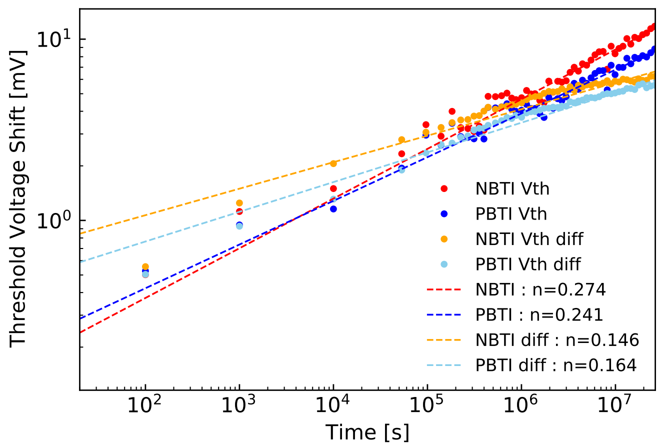


Fig. 6: Threshold voltage shifts and fitting results.

seconds are depicted in Figs. 7 and 8 respectively. Fig. 8 (b), a linear representation of Fig. 8 (a), highlights the variations observed during long-term measurements. After $1 \times 10^6$ seconds, the distribution becomes broad. Since environmental variations: such as changes in voltage or temperature does not change the distributions, the observed broadening cannot be attributed to environmental factors. Note that, only Fig. 7 is from a different chip. Long-term measurements were halted after two weeks when all ROs stopped oscillation. After that, the same chip was left at room temperature for one month, to recover from BTI-induced degradation. Then the chip was stored in the constant temperature oven again. Results for 1,000-second stress at temperatures of 100°C and 120°C are shown in Figs. 9 and 10 respectively. In Figs. 8, 9, and 10,

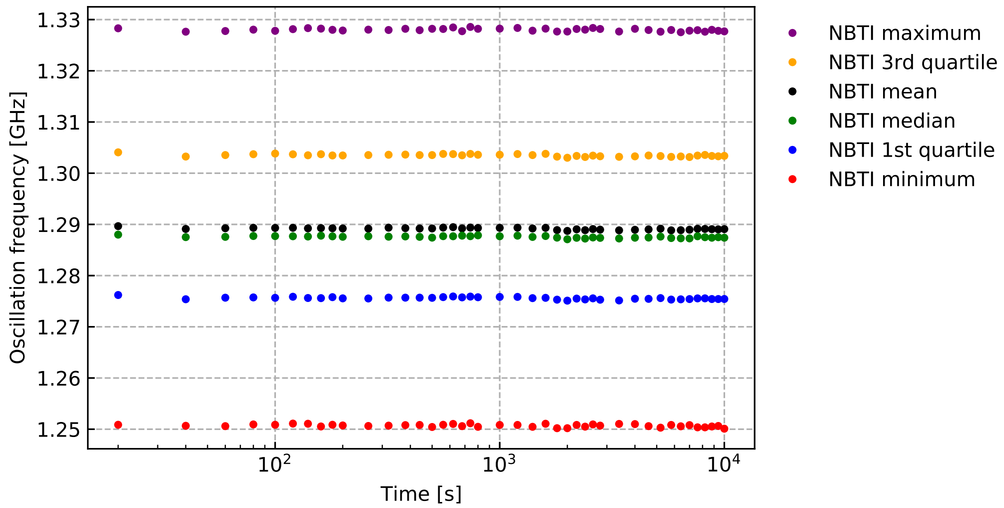


Fig. 7: Distributions of 840 NBTI-ROs in short-term measurement

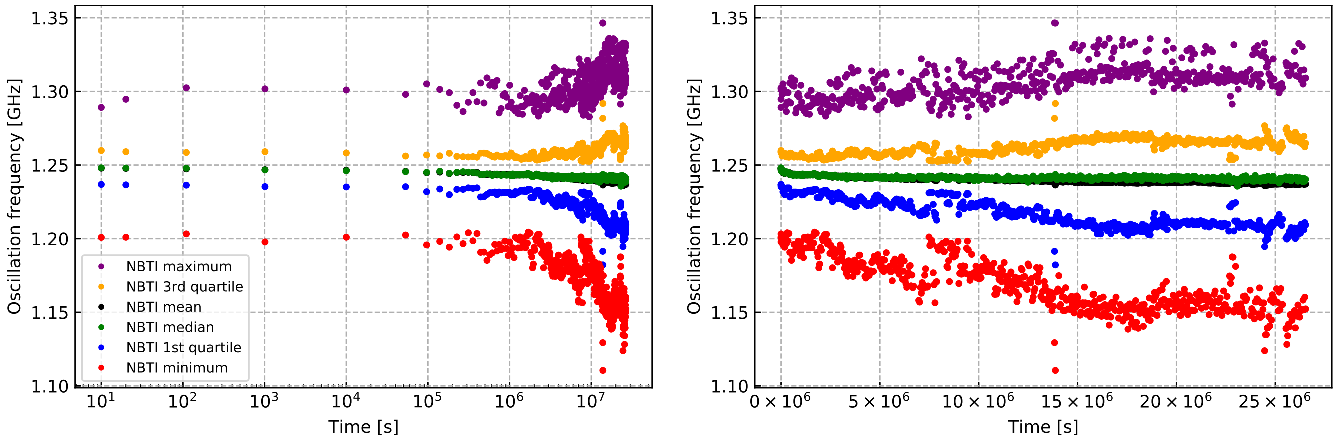


(a) Log-log plot distributions.

(b)Log-linear plot distributions.

Fig. 8: Distributions of 840 NBTI-ROs in long-term measurement.

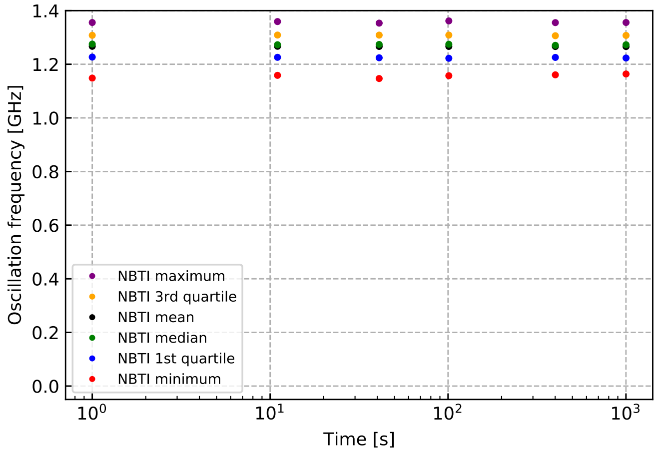


Fig. 9: Distributions of 840 NBTI-ROs at 100°C after 1 month recovery at room temperature

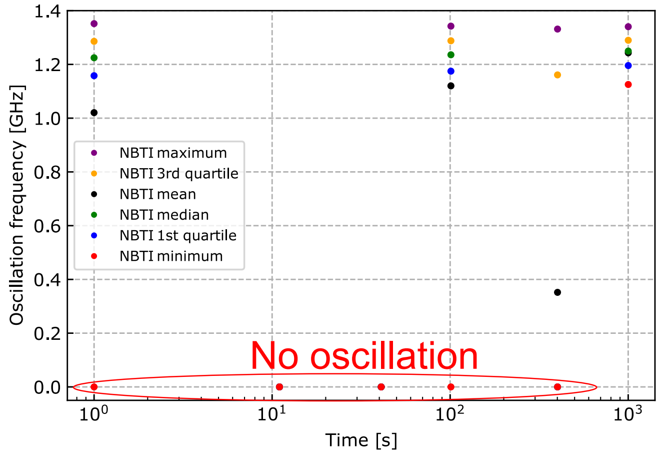


Fig. 10: Distributions of 840 NBTI-ROs at 120°C after 1 month recovery at room temperature

the same chip was used. While all ROs except non-oscillating ones functioned normally at 100°C, no oscillations occurred at temperatures above 120°C.

Hereafter, we discussed the distribution shift during the long-term stress. At 100°C, the distribution remained approximately 200MHz, indicating irreversible degradation from long-term stress. The distribution at 1,010 seconds is shown in Fig. 11. After 16 million seconds, the distribution becomes broad, as shown in Fig. 12. This wider distribution is attributed to intrinsic factors, since the environmental variations cannot alter the shape of the distributions.

Fig. 13 evaluates distribution using skewness and kurtosis. While skewness shows minimal variation over time, kurtosis decreases remarkably from $-0.4$ to $-1.2$. Considering that a Gaussian distribution exhibits a kurtosis of 0 while a uniform distribution exhibits a kurtosis of $-1.2$, these findings indicate that the long-term distribution is trending toward uniformity—likely as a result of the superposition of multiple Gaussian distributions, formally known as a Gaussian mixture distribution.

As shown in the Fig. 14, even the variations of the oscillation frequency of each RO becomes bigger as stress time. The variations started to become bigger after 1 million seconds. These individual variations are the primary contributors to the wider distributions.

Since each individual RO exhibits significant fluctuations,

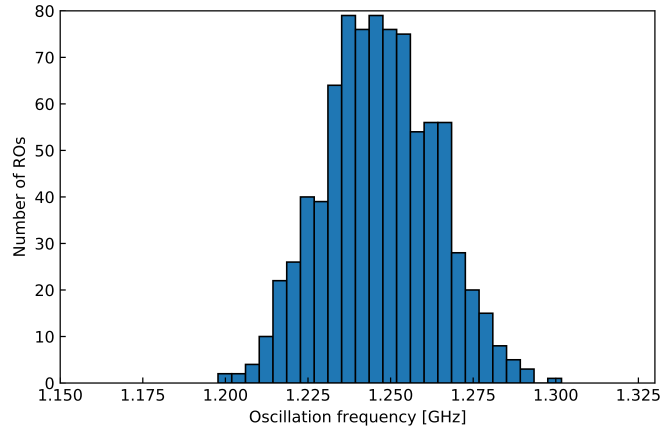


Fig. 11: Distributions of 840 NBTI-ROs at 1,010 s

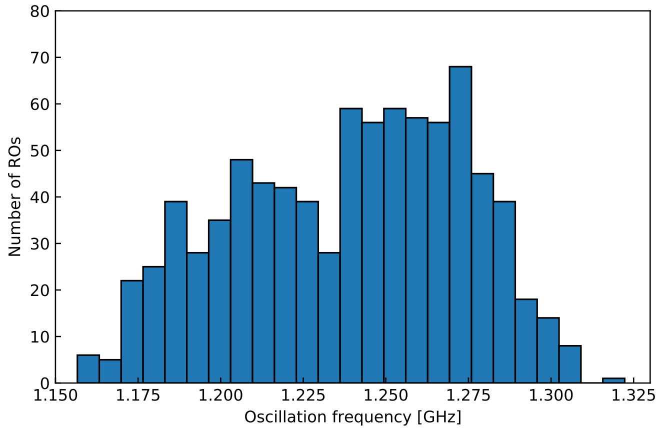


Fig. 12: Distributions of 840 NBTI-ROs at 16,728,410 s

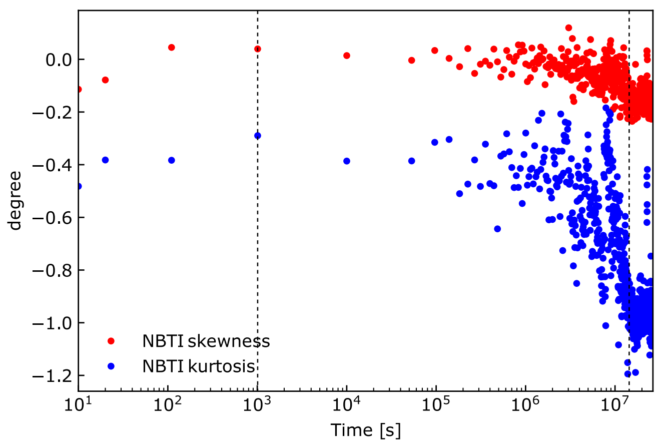


Fig. 13: skewness and kurtsis of 840 NBTI-ROs in long term measurement

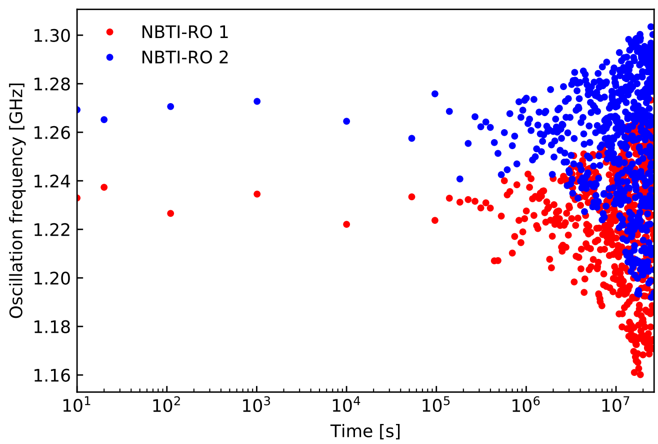


Fig. 14: Time variation in long-term measurements of four NBTI-ROs

RTN is likely one of the contributing factors [9]. Since this phenomenon is observed across all four types of ROs, it cannot be attributed to only BTI. After long-term stress, traps causing large Vth fluctuation become active. Those traps close to the gate terminal must be considered to estimate degradations after long periods.

## VI. Conclusion

BTI-induced degradation of 65 nm FDSOI ring oscillators (ROs) was measured using a long-term measurement system. Temperature and supply voltage were set to 125°C and a nominal voltage of 1.2V. The averaged BTI-induced degradation over 300 days follows a power-law function overall the time. Distributions of the results of 840 ROs at the initial phase has been changed from a Gaussian distribution at the short time to a Gaussian mixture distribution after the long period. This tendency comes from two different origins of degradations; defects close to the interface and those close to the gate. Although the averaged BTI-induced degradation follows a power-law function. It is important to clarify the distinction between short-term and long-term BTI-induced degradations.

During the long-term measurements, the distribution of 840 ring oscillators becomes broad. It can be caused by large Vth fluctuation from traps close to the gate terminal.

## Acknowledgment

The measurement chip used in this study was prototyped by Renesas Electronics Corporation and was supported by Synopsys Japan, Cadence Design Systems Japan, and Siemens EDA Japan through d.lab-VDEC at the University of Tokyo. We thank Dr. Mitsuhiko Igarashi, Dr. Shigetaka Kumashiro, Dr. Michitaro Yabuuchi, and Mr. Hironori Sakamoto of Renesas Electronics Corporation for their suggestions and comments.

## References

[1] V. Huard, C. Parthasarathy, C. Guerin, T. Valentin, E. Pion, M. Mammasse, N. Planes, and L. Camus, "NBTI degradation: From transistor to SRAM arrays," in *2008 IEEE International Reliability Physics Symposium*, April 2008, pp. 289–300.

[2] T. Matsumoto, K. Kobayashi, and H. Onodera, "Impact of random telegraph noise on CMOS logic circuit reliability," in *Proceedings of the IEEE 2014 Custom Integrated Circuits Conference*, 2014, pp. 1–8.

[3] R. Kishida, T. Asuke, J. Furuta, and K. Kobayashi, "Extracting Voltage Dependence of BTI-induced Degradation Without Temporal Factors by Using BTI-Sensitive and BTI-Insensitive Ring Oscillators," *IEEE Transactions on Semiconductor Manufacturing*, vol. 33, no. 2, pp. 174–179, 2020.

[4] K. Kobayashi, T. Kishita, H. Nakano, J. Furuta, M. Igarashi, S. Kumashiro, M. Yabuuchi, and H. Sakamoto, "Ultra Long-term Measurement Results of BTI-induced Aging Degradation on 7-nm Ring Oscillators," in *2023 IEEE International Reliability Physics Symposium (IRPS)*, 2023, pp. 1–7.

[5] P. F. Lu and K. A. Jenkins, "A built-in BTI monitor for long-term data collection in IBM microprocessors," in *2013 IEEE International Reliability Physics Symposium (IRPS)*, 2013, pp. 4A.1.1–4A.1.6.

[6] M. Bhushan and M.B. Ketchen, "Generation, elimination and utilization of harmonics in ring oscillators," in *2010 International Conference on Microelectronic Test Structures (ICMTS)*, 2010, pp. 108–113.

[7] "Failure Mechanism Based Stress Test Qualification for Integrated Circuits," in *AEC-Q100-Rev-H, Automotive Electronics Council*, Sept. 11, 2014, p. 3.

[8] S. Mahapatra, V. Huard, A. Kerber, V. Reddy, S. Kalpat, and A. Haggag, "Universality of NBTI - From devices to circuits and products," in *2014 IEEE International Reliability Physics Symposium*, June 2014, pp. 3B.1.1–3B.1.8.

[9] T. Grasser, *Noise in Nanoscale Semiconductor Devices*, Springer, 2020.